

# Maximizing information on the environment by dynamically controlled qubit probes

Analia Zwick,<sup>1</sup> Gonzalo A. Álvarez,<sup>1</sup> and Gershon Kurizki<sup>1</sup>

<sup>1</sup>Weizmann Institute of Science, Rehovot 76100, Israel

We explore the ability of a qubit probe to characterize unknown parameters of its environment. By resorting to quantum estimation theory, we analytically find the ultimate bound on the precision of estimating key parameters of a broad class of ubiquitous environmental noises (“baths”) which the qubit may probe. These include the probe-bath coupling strength, the correlation time of generic bath spectra, the power laws governing these spectra, as well as their dephasing times  $T_2$ . Our central result is that by optimizing the dynamical control on the probe under realistic constraints one may attain the maximal accuracy bound on the estimation of these parameters by the least number of measurements possible. Applications of this protocol that combines dynamical control and estimation theory tools to quantum sensing are illustrated for a nitrogen-vacancy center in diamond used as a probe.

## I. INTRODUCTION

Controlled spin- $\frac{1}{2}$  particles (qubits) are sensitive probes of the structure and properties of highly complex molecular, atomic or solid-state quantum systems. Novel quantum technologies requiring such high sensitivity at the nanoscale are based on qubit probes serving as sensors [1–8] or monitors of biological or chemical processes [9–11]. Here we focus on *the extraction of information characterizing the environment of a qubit probe*, by monitoring the decoherence process that the qubit undergoes [12]. Dynamical control, originally conceived as a tool for reducing decoherence effects [13–19], has also been shown to be a valuable source of information on environmental noises [10, 20–25]. This information is revealed by the dependence of the decoherence rate of the qubit probe on a control-field parameter, owing to the fact that, under weak coupling of the qubit and the environment (“bath”), this rate is universally expressed by the overlap of the environmental noise spectrum and a spectral filter function that is solely determined by the dynamical control [15–17, 26]. The filter function can then be designed by varying the control field to scan the noise spectrum. The information obtained from this procedure, dubbed “noise spectroscopy” [22, 23], is not only essential for designing the most effective (optimal) dynamical protection from decoherence caused by a given environment [26–33] of quantum-information processing [34–37], quantum-state transfer [38, 39], Hamiltonian engineering [24, 38, 40] and quantum-state storage [41, 42]. It may also become a means of understanding physical or chemical processes [9–11, 24] by analyzing their noise fluctuations in magnetic resonance spectroscopy and imaging with nanoscale resolution [6–8, 11, 43–45].

In order to further advance this promising noise spectroscopy and broaden its applicability, it is imperative to find *the best general strategy* for extracting the environmental (“bath-induced”) noise-spectrum information from the qubit-probe decoherence. The strategy we adopt aims at minimizing the error in estimating *key parameters* of the noise (bath) spectrum by measurements performed on the qubit probe (Sec. II). The minimal er-

ror is determined by the maximal quantum Fisher information (QFI) [46–49] gathered by measurements in the optimal basis (Sec. III). We here find (Sec. III A) the ultimate error bounds for unbiased estimators when the qubit probe, under arbitrary control, undergoes pure dephasing in the probe-bath weak-coupling regime. Motivated by practical experimental considerations and constraints, these ultimate bounds attain the best estimation precision by the least number of measurements possible. We achieve these goals by *replacing the free-evolution* (-induction) decay (FID) of the qubit state prior to each measurement by *dynamically-controlled evolution* designed to ensure the convergence to the ultimate error bound for the particular bath-spectrum parameter to be estimated (Sec. III B). For each such parameter, an appropriate filter-function must be generated by dynamical control (Sec. IV A) [17, 26]. We here focus on determining the general conditions that have to be satisfied for designing the filter function to attain the ultimate bounds.

The first step in the proposed strategy is the estimation of the coupling strength  $g$  of the bath to the probe, that can be interpreted as the noise variance. The proposed appropriate filter function is generated by *projections* onto an eigenstate of the  $\sigma_x$  probe-operator at a rate that conforms to the quantum Zeno regime [15, 24, 50] (Sec. IV B). This procedure, which *does not require prior knowledge of the bath spectral lineshape*, has been experimentally exploited to determine the coupling strengths of complex spin-networks without maximizing or optimizing the information obtained [24].

Once the coupling strength  $g$  is optimally estimated, the bath spectra have to be characterized by their normalized lineshapes. These spectra crucially depend on the bath correlation time  $\tau_c$  often unknown to us: it is typically the inverse of  $\omega_c$ , which is the width or the cutoff of the bath spectrum. We show that convergence to the lowest error bound on  $\tau_c$  is achievable through filter functions generated by common types of coherent dynamical-control sequences (Sec. IV C). By contrast, free-induction decay (FID) of the qubit coherence  $\langle \sigma_x(t) \rangle$  may preclude such convergence.

We further show for a family of generic baths that *optimized convergence requires a filter function that only samples (overlaps) a power-law region of the bath spectrum* (Sec. III B). Such spectral features *characterize omnipresent baths*: sub-Ohmic, Ohmic and super-Ohmic baths whose spectra obey a power-law at low frequencies, as well as noise spectra of generalized Ornstein-Uhlenbeck processes characterized by a power-law tail at high frequencies. These types of bath spectra are ubiquitous in solid-state, liquid or gas phases [11, 23, 51–53] where they represent collisional or diffusion processes [54, 55]. Other environmental parameters, such as spectral power-law exponents, the  $T_2$  decoherence time and diffusion coefficients, are shown to obey bounds analogous to those of  $g$  and  $\tau_c$  (Sec. IV D).

Finally, we demonstrate the practical feasibility of experiments that may attain the ultimate precision bounds by resorting to a real-time adaptive estimation protocol based on a Bayesian estimator and an online experimental learning design [56–59] (Sec. V). We resort to this protocol to illustrate the ability to achieve the predicted analytical bounds in an efficient way under experimentally relevant conditions, e.g. for nitrogen-vacancy center (NVC) probes in diamond [1–8, 45, 51]. Thus, the present analytical theory, supported by adaptive-estimation simulations, suggests that the proposed *synthesis of optimally-controlled noise spectroscopy and estimation theory* can become a powerful, broadly applicable, diagnostic tool (Sec. VI).

## II. DEPENDENCE OF THE QUBIT-PROBE DEPHASING ON AN UNKNOWN ENVIRONMENTAL PARAMETER

We consider a qubit-probe that experiences proper-dephasing by the environment (bath) under the action of the system-bath interaction Hamiltonian

$$H_{SB} = g\sigma_z B, \quad (1)$$

where  $g$  is the probe-bath interaction strength,  $\sigma_z$  is the appropriate Pauli operator for the probe and  $B$  is the bath operator (Fig. 1a). To obtain maximal information on the environment, a convenient initial probe-state is the symmetric superposition of the qubit-up/-down states in the  $\sigma_z$  basis,

$$\frac{1}{\sqrt{2}}(|\uparrow\rangle + |\downarrow\rangle) = |+\rangle, \quad (2)$$

and the optimal observable for the probe-state measurement is  $\sigma_x$  [49] (Appendix B). Our goal is to determine the dynamical control efficacy for estimating, one by one, the unknown parameters such as  $g$  and  $\tau_c$  that characterize the coupling bath spectrum.

We shall denote the particular bath parameter by  $x_B$ , and, accordingly, the bath coupling spectrum by  $G(x_B, \omega)$ . Under proper dephasing,

$$\langle \sigma_x(x_B, t) \rangle = \text{Tr}(\rho_S(x_B, t)\sigma_x) = e^{-\mathcal{J}(x_B, t)}, \quad (3)$$

where  $\mathcal{J}(x_B, t)$  is the attenuation factor due to dephasing. In the *probe-bath weak-coupling regime* known as the Born approximation for the bath, wherein the qubit-probe negligibly influences the environment [60], it obeys the universal formula (Appendix A) [15–17, 26]

$$\mathcal{J}(x_B, t) = \int_{-\infty}^{\infty} d\omega F_t(\omega)G(x_B, \omega), \quad (4)$$

where  $F_t(\omega)$  is a filter function which explicitly depends upon the dynamical control of the qubit-probe during time  $t$ .

This universal formula is exact for Gaussian noise. Yet it applies to any noise under the weak-coupling assumption in Eq. (4). In our bath-optimized control theory [15–17, 26, 27], the filter function is obtained to ensure optimal control for any given bath and task at hand. This theory does not impose any requirement on the temporal shape of dynamical control that defines the filter function: the control may be continuous or pulsed, coherent or projective, in contrast to the dynamical-decoupling formulation [14, 18, 29]. We stress that the optimal filter function obtained by this bath-optimized control theory does not require high-order corrections as opposed to dynamical decoupling control [26, 27].

The information about the unknown bath parameter  $x_B$  is encoded in the protocol defined by Eqs. (1)-(4) (Fig. 1a) by the probabilities  $p$  of finding the qubit in the  $|+\rangle$  (symmetric) or  $|-\rangle$  (antisymmetric) state when measuring  $\sigma_x$ . These probabilities obey

$$p(\pm|x_B, t) = \frac{1}{2} \left( 1 \pm e^{-\mathcal{J}(x_B, t)} \right). \quad (5)$$

## III. OPTIMAL ESTIMATION UNDER DYNAMICAL CONTROL

The minimum achievable relative error of the *unbiased* estimation of a single unknown parameter  $x_B$  is determined by the quantum Cramer-Rao bound to be

$$\varepsilon(x_B, t) = \frac{\delta x_B}{x_B} \geq \frac{1}{x_B \sqrt{N_m \mathcal{F}_Q(x_B, t)}}, \quad (6)$$

where  $N_m$  is the number of measurements and  $\mathcal{F}_Q(x_B, t)$  is the quantum Fisher information (QFI) that quantifies the maximum amount of information on  $x_B$  that can be extracted from a given state [46]. Therefore, we set out to maximize the information

$$\mathcal{F}_Q(x_B, t_{opt}) = \max_t \mathcal{F}_Q(x_B, t), \quad (7)$$

by choosing the optimal time  $t_{opt}$  to perform the measurement and an appropriate dynamical-control scheme (prior to the measurement), to obtain the minimal attainable (relative) error in the estimation of  $x_B$  for a given bath spectrum. For a qubit-probe obeying Eq. (5), the

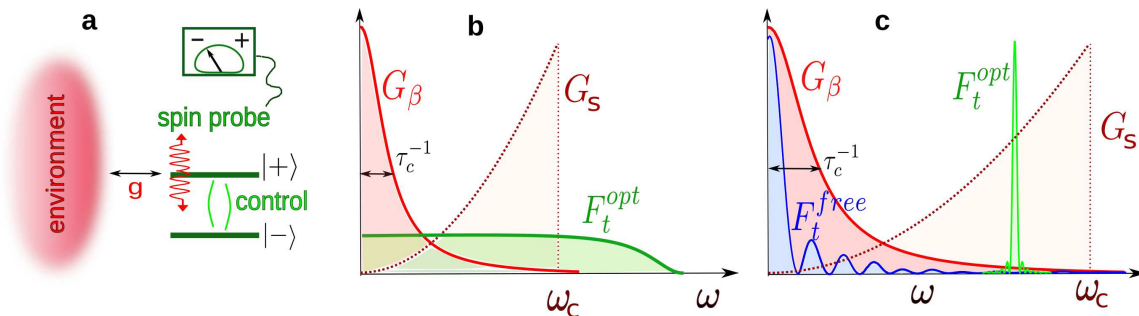


Figure 1: Scheme of noise-spectra parameter estimation. (a) Scheme of the probing process and its dynamical control: Dynamically controlled qubit-probe undergoes dephasing by the environment (bath). (b) An optimal qubit-probe filter function  $F_t^{opt}(\omega)$  generated by frequent projections is spectrally flat to the extent that it conforms to be quantum Zeno regime and allows the optimal determination of the coupling strength  $g$  regardless of the shape of  $S(\omega)$ . (c) A filter function of an optimally controlled qubit-probe,  $F_t^{opt}(\omega)$ , for obtaining the ultimate bound on the correlation time ( $\tau_c$ ) estimation. Such a filter must overlap only with the power-law tail of the Ornstein-Uhlenbeck noise spectrum  $S_\beta(\tau_c, \omega)$ , or with  $\omega > 0$  but not with  $\omega_c$  for the (super) Ohmic spectrum  $S_s(\tau_c, \omega)$ . The free-evolution (FID) filter function  $F_t^{free}(\omega)$  does not fulfill the requirements for achieving the bound, since it is centered at  $\omega = 0$ .

QFI is gathered by measurements in the optimal basis (Appendix B)

$$\mathcal{F}_Q(x_B, t) = \frac{e^{-2\mathcal{J}(x_B, t)}}{1 - e^{-2\mathcal{J}(x_B, t)}} \left( \frac{\partial \mathcal{J}(x_B, t)}{\partial x_B} \right)^2. \quad (8)$$

From this expression, the QFI maximum is obtained by finding the optimal tradeoff between the signal-amplitude contrast (the magnitude of  $\frac{e^{-2\mathcal{J}}}{1 - e^{-2\mathcal{J}}}$ ) and the sensitivity of the signal-attenuation to the parameter  $x_B$  (the derivative  $\frac{\partial \mathcal{J}}{\partial x_B}$ ). Obviously, neither should be too small if Eq. (8) is to be maximized. Their optimal tradeoff determines  $t_{opt}$  for a given control scheme (Fig. 2a). To evaluate the efficacy of different dynamical controls in attaining the highest accuracy in  $x_B$ , we then use the error (6) at  $t_{opt}$ , *i.e.*  $\varepsilon(x_B, t_{opt})$ , as the figure of merit.

We focus here on the ultimate error bounds for the estimation precision *per measurement* for the qubit-probe that undergoes pure dephasing within the weak-coupling regime. These bounds are of practical importance in typical experimental situations where the initialization and readout times, normally determined by  $T_1 \gg T_2$ , constrain the time interval between measurements.

Alternatively, in instances where  $T_1$  is not the dominant constraint, one may be interested in the ultimate precision bound attainable during a given interrogation time that extends over many measurements,  $T = N_m t$ . In such cases the Fisher information *per unit time* has to be maximized:

$$\mathcal{F}_Q(x_B, t_{opt})/t_{opt} = \max_t (\mathcal{F}_Q(x_B, t)/t). \quad (9)$$

### A. Ultimate estimation bounds

As discussed below, a broad class of practically relevant environmental noise processes cause the attenuation factor  $\mathcal{J}(x_B, t)$  to have a power-law dependence in  $x_B$  with

an exponent  $\alpha$ , where the derivative of  $\mathcal{J}(x_B, t)$  is tightly bounded by its value in the power-law region, as

$$\left| \frac{\partial \mathcal{J}(x_B, t)}{\partial x_B} \right| \leq \frac{\alpha \mathcal{J}(x_B, t)}{x_B}. \quad (10)$$

The equality strictly holds when  $\mathcal{J}(x_B, t)$  is an *homogeneous function of degree  $\alpha$*  for the parameter  $x_B$ .

The bound (10) leads to a tight lower bound on the relative error in (6), which holds for *either free decay (FID) or arbitrary dynamical control* of the probe coherence (Appendix C)

$$\varepsilon(x_B, t) \geq \frac{\sqrt{1 - e^{-2\mathcal{J}_0}}}{\alpha \sqrt{N_m} \mathcal{J}_0 e^{-\mathcal{J}_0}} = \frac{\varepsilon_0}{\alpha \sqrt{N_m}}. \quad (11)$$

Here the value of  $\mathcal{J} = \mathcal{J}_0$  that minimizes this bound,  $\mathcal{J}_0 = 1 + \frac{1}{2}W(-2e^{-2}) \approx 0.8$ ,  $W(z)$  being the Lambert function, yields the equality in (11), with  $\varepsilon_0 \approx 2.48$ . We have thus obtained a *universal, ultimate error bound for the unbiased estimation of  $x_B$  in a broad class of noise spectra* probed by a qubit-probe undergoing dephasing within the probe-bath weak-coupling regime.

### B. Key parameter estimation

This general bound applies to the estimation of any parameters that satisfy  $\mathcal{J}(x_B, t) \propto x_B^{\pm\alpha}$ . We here discuss in detail some examples of estimating key parameters that belong to this class in typical scenarios of practical importance:

(i) The effective coupling strength  $g$  of the qubit-probe with the dephasing bath is required for defining

$$G(x_B = g, \omega) = g^2 S(\omega), \quad (12)$$

$S(\omega)$  being the normalized spectral density of the bath autocorrelation function, so that  $G(g, \omega)$  and  $\mathcal{J}(g, t)$  are

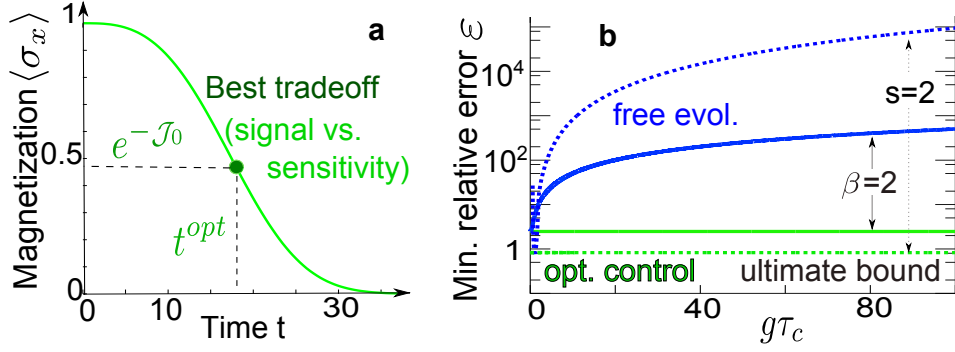


Figure 2: Optimization for achieving the ultimate precision bound. (a) Magnetization  $\langle \sigma_x \rangle$  as a function of the measurement time  $t$  of a qubit-probe experiencing dephasing due to Ornstein-Uhlenbeck process, with Lorentzian spectrum  $G_{\beta=2}(\tau_c=10, \omega)$  with  $g=1$  under a CPMG control sequence with  $N=8$  pulses using the exact analytical expression derived from Eq. (4) [11]. The optimal time  $t^{opt}$  that determines the best tradeoff between the signal contrast (almost halfway between 0 and 1) and the highest sensitivity of the decay rate to  $\tau_c$ , provides the most accurate estimation of  $\tau_c$ . (b) Minimal relative error  $\varepsilon(\tau_c, t^{opt})$  per measurement ( $N_m=1$ ) of the estimation of  $\tau_c$  as a function of  $g\tau_c$  for a Lorentzian spectrum  $G_{\beta=2}(\tau_c=10, \omega)$  (dashed lines) and a super-ohmic spectrum  $G_{s=2}(\tau_c=10, \omega)$  (solid lines) calculated from the integral of Eq. (4), both with  $g=1$ . The minimal relative error under optimal control (CPMG/CW with  $N$  pulses/cycles satisfying the conditions given in the main text, green lines) achieves the ultimate bounds ( $\frac{\varepsilon_0}{3\sqrt{N_m}}$  (dashed-) and  $\frac{\varepsilon_0}{\sqrt{N_m}}$  (solid-) green lines for  $s=2$  and  $\beta=2$  respectively). It can improve the best precision obtainable under free-evolution (blue lines) by several orders of magnitude.

homogeneous functions of degree  $\alpha=2$  in  $g$ .

(*iii*) The correlation time  $\tau_c$  of noise fluctuations is required for describing generalized Ornstein-Uhlenbeck processes, with normalized spectral densities

$$S_\beta(x_B=\tau_c, \omega) = \mathcal{A}_\beta \frac{\tau_c}{1 + \omega^\beta \tau_c^\beta}, \quad (13)$$

where  $\beta \geq 2$  is an even integer and  $\mathcal{A}_\beta = \frac{\beta}{2\pi} \sin(\frac{\pi}{\beta})$  is the normalization factor.

(*ii*) The correlation time  $\tau_c = \omega_c^{-1}$ , that is the inverse of the cutoff frequency  $\omega_c$ , in generalized Ohmic spectra

$$S_s(x_B=\tau_c, \omega) = (s+1)\omega_c^{-(s+1)}\omega^s \Theta(\omega)\Theta(\omega - \omega_c), \quad (14)$$

where  $\Theta(\omega)$  is the step function,  $s=1$  stands for a Ohmic spectrum,  $0 < s < 1$  for a sub-Ohmic spectrum, and  $s > 1$  for its super-Ohmic counterpart.

Both spectral densities (13) and (14) satisfy  $\left| \frac{\partial S}{\partial \tau_c} \right| \leq \frac{\alpha S}{\tau_c}$ , and consequently the bound (10). Furthermore, both spectra attain the ultimate bound (11) at frequency ranges where they have power-law dependence (Appendix C): spectral density (13) at high frequencies, where it becomes a homogeneous function of degree  $\alpha = \beta - 1$ , and spectral density (14) at low frequencies, when we restrict ourselves to  $\omega < \omega_c$  to avoid the cutoff effects, thus rendering the spectral density a homogeneous function of degree  $\alpha = s + 1$ .

(*iii*) The dephasing time  $T_2$  in the attenuation exponent which is a homogeneous function of degree  $\alpha$ ,  $\mathcal{J}(x_B = T_2, t) = (t/T_2)^\alpha$ , may be estimated down to the ultimate bound.

## IV. DYNAMICAL CONTROL STRATEGIES FOR ACHIEVING THE ULTIMATE BOUND

### A. Achieving the ultimate-bound by dynamical control

It follows from the discussion above that the ultimate error bound, Eq. (11), in the estimation of  $x_B = g$  or  $\tau_c$ , can be attained provided that the dynamical control on the probe generates a filter  $F_t(\omega)$  that extends only over the frequency band where the noise spectrum behaves as a power-law in  $x_B^{\pm\alpha}$  and the equality in Eq. (10) is fulfilled. Then, upon adjusting the total control time such that  $\mathcal{J}(x_B, t^{opt}) = \mathcal{J}_0$ , the equalities in Eq. (11) are also fulfilled.

We note that these are general conditions for attaining the ultimate error bound per measurement, but they do not invoke the optimization of the filter function under specific constraints that may be imposed in a given experimental setup. In such setups further optimization is required to approach as best we can the ultimate error bounds.

### B. Estimating the probe-bath interaction strength $g$

If  $S(\omega)$  is *unknown* apart from a crude estimate of its overall width, dynamical control is needed for estimating  $g$  down to the ultimate precision bound. The appropriate control is such that the filter function  $F_t(\omega) = F_t$  is flat in the domain of  $S(\omega)$ , leading to an attenuation factor  $\mathcal{J} = F_t g^2$  that is independent of the noise spectrum. For free evolution this limit holds when the interval is much shorter than the correlation time  $\tau_c$  of the environment, so that the qubit-probe evolves freely (Appendix D). This

condition can only be fulfilled for large enough  $\tau_c$ .

To overcome this limitation, we may instead realize such a filter at times larger than  $\tau_c$  via repeated stroboscopic projections of the qubit-probe in the basis of  $|\pm\rangle$ , *i.e.* by quantum non-demolition (QND) measurements at a rate that is high enough to conform to the quantum Zeno regime [50]. The filter function then describes spectral broadening of the  $|\pm\rangle$  eigenvalues far beyond the width of  $S(\omega)$  (Fig. 1b). The attenuation factor is then [15, 17, 24] (Appendix D)

$$\mathcal{J}_{\text{Zeno}}(g, t) = \frac{g^2 t^2}{2N}, \text{ if } \frac{t}{N} \ll \tau_c, \quad (15)$$

obtained for  $N$  QND measurements during the total control time  $t$ . The advantage of this Zeno regime is that it requires  $\frac{t}{N} \ll \tau_c$ , rather than the total time  $t$ , to be less than  $\tau_c$ . Since the outcomes of these measurements *need not be read out*, but rather used to guide the evolution, they may be *emulated* by impulsive noise-induced dephasing of the qubit probe that has the same effect as a projection on the probe evolution [17, 24, 61]. This QZE regime has been already exploited experimentally to determine the coupling strengths of complex spin-networks [24].

Under the quantum-Zeno condition of (15), the error estimation bound (11) is achieved when the total control time (after which  $\sigma_x$  is measured and read out - see (5)) is chosen to have the optimal value

$$t_{\text{Zeno}}^{\text{opt}} = \frac{\sqrt{2N\mathcal{J}_0}}{g}, \text{ provided that } N \gg \frac{2\mathcal{J}_0}{g^2\tau_c^2}. \quad (16)$$

This equation (further discussed in Appendix D) constitutes the main condition on an optimal filter designed to estimate  $g$ .

### C. Estimating the correlation time $\tau_c$

To achieve the ultimate precision bound (11) for the estimation of  $\tau_c$  of noise spectra (13)-(14), the control on the probe should generate a filter  $F_t(\omega)$  that only overlaps with the power-law portion of  $S_{\beta(s)}(\tau_c, \omega) \propto \tau_c^{\mp\alpha} \omega^{\mp(\alpha\pm 1)}$ , as shown in Fig. 1c. By contrast, FID of the probe coherence generates a filter (sinc) function centered at zero frequency, thus *preventing the bound* in Eq. (11) *from being reached*.

While various controls may allow the best estimation according to Eq. (11), we here analytically study the conditions for achieving the ultimate bound under standard CPMG sequences of  $\pi$  pulses [62], or under *continuous-wave driving* (CW). In control sequences of equidistant pulses  $N \gg 1$ , the filter function  $F_t(\omega)$  converges to a sum of delta functions (narrowband filters) centered at the harmonics of the inverse CPMG time period, while for CW there is a single frequency component [17, 23, 30] (Appendix D). In the following we use these filter functions, to analytically infer the required total control time

$t$  and  $N$  that allow the bound to be attained for the two classes of power-law spectra in Eqs. (13) and (14) (see Appendix D for details):

(i) For *generalized Ornstein-Uhlenbeck spectra*  $S_{\beta}(\omega)$ , only high frequencies must be probed by the dynamical control filter. To this end, the intervals between pulses or refocusing periods must obey  $\frac{t}{N} \ll \tau_c$ . Then,  $\mathcal{J}_{\beta} \propto \tau_c^{-(\beta-1)}$  satisfies the equality in (11) and the minimal relative error attains the ultimate bound, provided that the total control time is chosen to have the optimal value

$$t_{\beta}^{\text{opt}} = \tau_c^{\beta+1} \sqrt{\frac{N^{\beta} \mathcal{J}_0}{c_{\beta} g^2 \tau_c^2}}, \quad (17)$$

where  $c_{\beta}$  is a constant depending on the control sequence. The bound can be attained only if  $N$  is sufficiently large to satisfy  $t_{\beta}^{\text{opt}}, \tau_c \gg \frac{t_{\beta}^{\text{opt}}}{N}$  and only overlaps with the power-law tail, as shown in Fig. 1c. By contrast, FID fails this condition, since its filter mainly overlaps with  $\omega \approx 0$  (Fig. 1c), causing a larger error in the estimation, as shown in Fig. 2b.

(ii) For *generalized Ohmic spectra*  $S_s$ , the filter should only overlap with the noise spectrum at a frequency lower than the cutoff,  $0 < \omega < \omega_c$ , avoiding any overlap at  $\omega_c$ . Then,  $\mathcal{J}_s \propto \tau_c^{s+1}$  satisfies the equality in (11) and the minimal relative error attains the ultimate-bound when the measurement of  $\sigma_x$  is performed at the optimal total control time

$$t_s^{\text{opt}} = \tau_c^{s-1} \sqrt{\frac{c_s g^2 \tau_c^2 N^s}{\mathcal{J}_0}}. \quad (18)$$

Here  $\frac{t_s^{\text{opt}}}{N} > \tau_c$ , and  $N \gg 1$  ensure the filter is narrowband with negligible tail at  $\omega_c$ , as opposed to its free-evolution (FID) counterpart that causes a much larger estimation error (see Fig. 2b).

Equations (17) and (18) thus constitute our main condition on the *optimal filter design* for estimating  $\tau_c$ .

### D. Power-law estimation

One can *optimally estimate the exponent*  $\beta$  or  $s$  that governs the bath spectrum by maximizing the QFI (8) for the estimation of  $x_B = \gamma = \beta + 1 = 1 - s$  (Appendix D). This maximization leads to the ultimate precision bound

$$\varepsilon(\gamma, t) \geq \frac{1}{\gamma \sqrt{N_m \mathcal{F}_{\mathcal{Q}}(\gamma, t)}} \geq \frac{\sqrt{1 - e^{-2\mathcal{J}_1}}}{\sqrt{N_m} \mathcal{J}_1 |\ln(\mathcal{J}_1)| e^{-\mathcal{J}_1}} = \frac{\varepsilon_1}{\sqrt{N_m}}, \quad (19)$$

with  $\mathcal{J}_1 = e^{-2.246} \approx 0.106$  and  $\varepsilon_1 \approx 2.04$ . The bound is achieved when the qubit only probes the power-law regime of noise spectra (13)-(14). Provided that the CPMG or CW dynamical control probes the power law region, the bound is attained when the qubit-probe is measured at

$$t_{\text{opt}} = T_2 \sqrt[3]{\mathcal{J}_1}, \quad (20)$$

where  $\mathcal{J}(\gamma, t) = \left(\frac{t}{T_2}\right)^\gamma$  and  $T_2$  is the dephasing time (that depends on the applied control).

## V. REAL-TIME ESTIMATION PROTOCOL

The predicted optimal time  $t^{opt}$  for performing a measurement following the dynamical control or FID of the quantum-probe coherence, explicitly depends on the *unknown parameter*  $x_B$  to be estimated (see Eqs. (16), (17), (18) and (20)). In practice, one may bypass this difficulty by *estimating  $x_B$  and simultaneously finding the optimal time* to monitor the probe via an efficient real-time estimation protocol [56, 57, 59]. We illustrate here the implementation of this protocol and show that it attains the predicted ultimate bound (11) if the qubit-probe is optimally controlled.

The protocol is based on a Bayesian estimator and an online experimental learning design that maximizes the information gain, similar to the one that was recently implemented for improving the suppression of decoherence in quantum dots [58]. Its stages are as follows:

(i) We initially guess a probability distribution  $p(x_B)$  for the unknown parameter  $x_B$  that represents our apriori knowledge of the parameter to be estimated. Physically, we should have  $x_B > 0$ , and therefore one can assume a flat distribution of  $p(x_B)$ ,  $x_B \in (x_B^{min}, x_B^{max}]$  that contains the true value  $x_B^{true}$ .

(ii) We then determine the best time  $t_m$  to perform a measurement for maximizing the information gain about  $x_B$  which is defined by the information entropy  $U(t_m) = \max_t \{U(t)\}$  (Appendix E), which depends on  $p(x_B)$  and the likelihood function  $p(d|x_B, t)$  of Eq. (5) that determines the conditional probability to obtain the possible outcome data of the measurement  $d = \{+, -\}$ .

(iii) We next perform a measurement of  $\sigma_x$  of the qubit-probe state, initialized in the state  $|+\rangle$ , at the optimal time  $t_m$ , obtaining the outcome data  $d$  with probability  $p(d|x_B^{true}, t)$ . According to the obtained data, we update our knowledge of  $x_B$  by the Bayesian Rule

$$p^{new}(x_B) \equiv p(x_B|d, t_m) = \frac{p(d|x_B, t_m)p(x_B)}{p(d|t_m)}, \quad (21)$$

where  $p(d|t)$  is a normalization factor for integration over  $x_B$ .

The estimation of  $x_B$  improves upon iteratively repeating this three-stage process  $N_m$  times,  $N_m$  standing for the number of measurements. When an adequate control is chosen, the probability distribution  $p(x_B)$  converges to a narrow peak around  $x_B^{true}$ . By contrast, the convergence under free-evolution can be very poor.

Figure 3 presents a simulated experiment of this iterative process for the estimation of  $g$  and  $\tau_c$  of the environmental noise by a NVC spin-probe in two types of diamond samples whose intrinsic environmental characteristics require dynamical control to attain the ultimate bound (11):

(a) We simulate the estimation of  $\tau_c$  for the NVC-probe evolving freely (undergoing FID), as compared to it being nearly optimally controlled by a CPMG sequence with  $N = 8$  subject to an Ornstein-Uhlenbeck process characterized by  $G_{\beta=2}(\tau_c^{true} = 10\mu s, \omega)$  with  $g = 1$  MHz (consistently with the HPHT diamond sample data of Ref. [51]). Our simulated best-measurement timings  $t_m$  converge to the theoretically predicted  $t^{opt}$  that maximizes the QFI (8), as exemplified in Fig. 3a for CPMG control, where  $t^{opt} \approx 18.25\mu s$  is on time scales compatible with the accessible experimental times [51]. Concurrently, the minimum relative error converges to  $\varepsilon(\tau_c, t_{opt})$  predicted from the Cramer-Rao bound (Fig. 3b).

(b) In Fig. 3c we simulate the estimation of  $g$  under similar conditions by a sequence of  $N = 500$  QND measurements due to induced dephasings whose optimal intervals are  $\frac{t^{opt}}{N} \approx 1.9\mu s$  and compare these results to the FID results. In this case  $G_{\beta=2}(g^{true} = 0.03\text{MHz}, \omega)$  with  $\tau_c = 10\mu s$  is consistent with the spectral density determined in Ref. [51] for the  $^{12}\text{C}$  diamond sample. This estimation procedure is performed *without assuming the lineshape of the spectral density*. It is seen from Fig. 3c that the precision error eventually saturates for the free evolution (FID) at a precision that is limited by our lack of knowledge of the lineshape. By contrast, this saturation can be overcome in the QZE regime achieved by projective measurements.

The foregoing simulations have thus confirmed, under experimentally realistic conditions, our second major analytical result, whereby the *ultimate theoretical bound* (11) is *indeed attainable under optimal control, but hardly ever under free-evolution*.

## VI. DISCUSSION

We have demonstrated that dynamical control of a quantum probe not only *dramatically improves* the quantum estimation of environmental parameters compared to the free-evolution (induction) decay (FID) of its coherence: it may be *imperative* to use such control, since FID may preclude their correct estimation. In particular, for generic noise spectra, as in generalized Ornstein-Uhlenbeck and Ohmic processes, the ultimate analytical bounds for the coupling strength and correlation-time estimation precision derived here can be achieved by optimizing the dynamical control on the probe. The optimal controls suitable for the estimation of  $g$ ,  $\tau_c$  (Fig. 1, 3) or the power-law exponent are generally different, but the protocol is similar. Specifically, we demonstrated that the ultimate estimation bound for  $g$  can be attained in the quantum Zeno regime without prior knowledge of the environmental spectral-density shape. Once this probe-environment coupling is known, the environmental correlation time can be reliably estimated by standard dynamical-control sequences.

Experimental conditions typically require a minimized average error within the coherence time interval shown

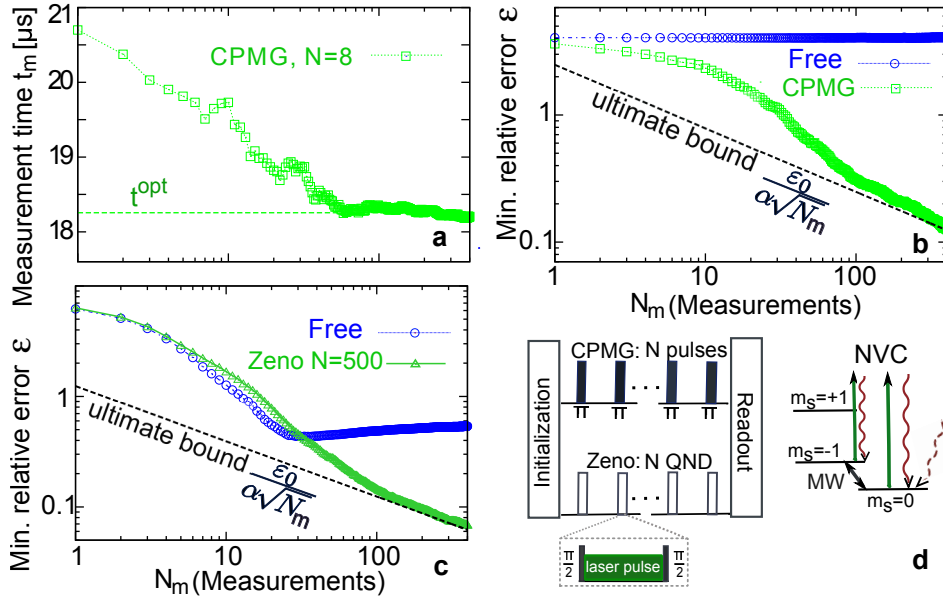


Figure 3: Simulation of a experimental real-time adaptive estimation protocol for realistic conditions with a NVC spin-probe. (a,b) Convergence of the real-time adaptive estimation protocol to the theoretically predicted values for estimating  $\tau_c$ . Free-evolution of the probe (blue circles) is contrasted with that of a dynamically controlled probe under CPMG (green square) sequence with  $N = 8$  in the presence of an Ornstein-Uhlenbeck process with Lorentzian spectrum  $G_{\beta=2}(\tau_c^{true}=10\mu s, \omega)$ , with  $g = 1$  MHz consistently with the spectral density of a HPHT diamond sample determined in Ref. [51]. The simulated curves derived from exact analytical results of Eq. (4) [11], were averaged over 600 realizations. In (a) the optimal measurement time  $t_m$  as a function of  $N_m$  converges to the value  $t^{opt}$  for the CPMG case. Similar curves converging to the corresponding  $t^{opt}$  are observed for other controls and free evolution. In (b) the minimal relative error  $\varepsilon(\tau_c, t^{opt})$  converge to the (Cramer-Rao) bound. Under free evolution the regime where  $\varepsilon \propto \frac{1}{\sqrt{N_m}}$  is attained for  $N_m \gg 100$ . The *ultimate bound* ( $\frac{\varepsilon_0}{\alpha\sqrt{N_m}}$  dashed line,  $\alpha = \beta - 1$ ) is only attained by optimal control. (c) Convergence to the minimal relative error  $\varepsilon(g, t_{opt})$  to the (Cramer-Rao) bound for estimating  $g$  by  $N = 500$  consecutive projective measurements in the Zeno regime (green triangle) compared to the estimation under free evolution (blue circle). In this case  $G_{\beta=2}(g=0.03\text{MHz}, \omega)$ , with  $\tau_c = 10\mu s$ , consistently with the spectral density of a  $^{12}\text{C}$  diamond sample determined in Ref. [51]. Here too the *ultimate bound* ( $\frac{\varepsilon_0}{2\sqrt{N_m}}$  dashed line,  $\alpha = 2$ ) is only attained by optimal control. (d) Proposed scheme for using a NVC as a qubit-probe for its environment. The  $m_s = 0$  ( $|0\rangle$ ) state is fully populated by laser irradiation (dashed curly arrow). Microwave (MW) pulses are selectively applied between the states with  $m_s = 0$  and  $-1$  ( $|0\rangle$  and  $|-1\rangle$ ) to initialize the spin-probe in a  $|+\rangle = \frac{1}{\sqrt{2}}(|0\rangle + |-1\rangle)$  state, and to apply the  $\pi$  pulse CPMG sequence for estimating  $\tau_c$ . For estimating  $g$ , projective measurements are performed by combining MW  $\pi/2$  pulses on the  $0 \leftrightarrow -1$  transition and laser-induced relaxation between the ground and excited electronic states that conserve the spin components (solid curly arrows). The readout is done at the end of the sequence by detecting the laser-induced fluorescence signal.

in Fig. 2b, if this interval is much shorter than the combined post-measurement readout and initialization time of the qubit. Under such conditions, an important implication of the present analysis is that it yields the optimal *total time* of the pre-measurement dynamical control and thereby the *number of pulses* and the delay between them that need be applied to attain the best precision per measurement. However, in the (rarely encountered) opposite limit of fast readout and initialization, the overall error rate of the measurements is to be minimized. Then, a similar optimization can be performed by maximizing the Fisher information *per unit time*. If additional specific constraints are imposed by a particular experimental setup, e.g. limited power or estimation time, then further optimization is needed to find the optimal filter function. In such cases, the goal would be to approach as best we can the ultimate error bound under the given constraints.

A real-time adaptive estimation protocol has illustrated the ability to find the optimal time of dynamical control for achieving the predicted precision bounds, e.g., for a nitrogen vacancy center (NVC) in a diamond that acts as a qubit-probe of the bulk or surface in optically detected NMR and MRI. Its aim here is to determine the noise spectrum generated by nuclear or electronic spins [6–8, 44, 45], as well as other sources of dephasing. In Fig. 3 we illustrated this protocol for estimating both  $g$  and  $\tau_c$  near an NVC used as a probe. The inferred correlation times of the noise fluctuations can be particularly helpful for studying molecular diffusion at the nanoscale, where the power law tails of noise spectra allow the extraction of the diffusion rates and restriction lengths associated with pore structures and thereby characterizing biological processes [11, 43].

In other scenarios, power-law tails can also characterize

charge diffusion in conducting crystals [55] or spin diffusion in complex spin-networks [23, 24, 54, 63]. Generalized Ohmic spectra may help understanding the functioning of nanoscale electromechanical devices [64], as well as superconducting devices attached to conducting leads [65].

Several extensions of the outlined strategy will be further explored:

(a) If uncontrollable noise sources are present, such as an intrinsic  $T_2$  decoherence due to a white-noise (Markovian) process or due to pulse imperfections, we may have to resort to more elaborate controls, nicknamed by us “selective dynamical recoupling” (SDR), which we have shown to allow *selective* probing of the targeted noise source [10, 11]. SDR was already implemented to *selectively* monitor diffusion processes characterized by an Ornstein-Uhlenbeck spectral density, so as to determine the probe-environment coupling strengths [10, 66] and the environmental correlation time, as well as diffusion restriction lengths [11, 43] in systems of biological and chemical interest. We envisage that by incorporating SDR within the present optimized estimation strategy one may eliminate Markovian (intrinsic- $T_2$  and pulse-error) effects and allow a clean parameter estimation of the targeted noise spectrum.

(b) A qubit-probe may be replaced by an entangled  $n$ -particle probe that may yield a lower error bound [67–69]. The estimation strategy will remain similar, but the dynamical control will have to be adapted to a multipartite scenario, based on the approach of Refs. [26, 70, 71].

(c) The present strategy, whereby environmental parameters are estimated one by one, provides the ultimate precision bounds that can be attained for estimating a single parameter, assuming that the remaining parameters are known with much better accuracy. Therefore, these bounds are also valid for more elaborate multiparameter estimation strategies based on a quantum Fisher information matrix [72], although these bounds may not be tight in the latter case. Still, the single-parameter estimation expounded here may be superseded by multiparameter optimized estimation per measurement.

To conclude, we have analytically set the error bounds on environmental-parameter estimation and demonstrated the ability to extract such environmental information with maximal accuracy by the least number of measurements possible upon invoking dynamical control. This general result for a qubit-probe weakly coupled to its environment opens the door to the development of an important diagnostic tool of environmental processes by quantum probes.

## Appendix A: Anamnesis: Filter function derivation for qubit probe under dephasing (Following Refs [14-16,24-25])

The Hamiltonian of a single spin-probe interacting with a bath that produces pure dephasing is

$$H = H_S(t) + H_B + H_{SB}, \quad (\text{A1})$$

with

$$H_S = \frac{\omega_0}{2}\sigma_z + f(t)e^{-i\omega_0 t}\sigma_x, H_{SB} = S \otimes B = g\sigma_z B, \quad (\text{A2})$$

where  $f(t)$  is the dynamical control applied to the qubit,  $B$  and  $S$  are the operators of the bath and the system ( $\sigma_z$  for pure dephasing) respectively, and  $g$  is their coupling strength.

In the interaction picture the Hamiltonian can be written as

$$H_{SB}^I(t) = S(t) \otimes B^\dagger(t), \quad (\text{A3})$$

where

$$\begin{aligned} S(t) &= U_S^\dagger(t) S U_S(t), U_S(t) = \mathcal{T} e^{-i \int_0^t dt' H_S(t')}, \\ B(t) &= U_B^\dagger(t) B U_B(t), U_B(t) = e^{-i H_B t}. \end{aligned} \quad (\text{A4})$$

Therefore, Eq. (A3) becomes

$$H_{SB}^I = g\Omega(t)\sigma_z B(t), \quad (\text{A5})$$

where  $\Omega(t)$  is the dynamical control rate of the system.

From this form one can derive the non-Markovian master equation for the density matrix of the system,  $\rho_S(t)$  in the interaction picture, which in the Born approximation one assumes a weak coupling  $g$  such that the influence of the qubit-probe on the environment is small (usually called the weak-coupling approximation). In this approximation, the density matrix of the environment  $\rho_B$  is only negligibly affected by the interaction with the qubit-probe, and the state of the total system at time  $t$  is allowed to be expressed as  $\rho(t) \approx \rho_S(t) \otimes \rho_B$  [60]. The resulting non-Markovian master equation is then given by [15–17, 73, 74]

$$\dot{\rho}_S(\tau_c, t) = \int_0^t dt' \{g^2 \Phi(x_B, t-t') [S(t'), S(t) \rho_S(t)] + h.c.\}, \quad (\text{A6})$$

where  $\Phi(x_B, t'-t'') = \text{Tr}_B \{B(t'-t'') B(0) \rho_B(0)\}$  are the bath correlation functions and  $x_B$  is a parameter that characterizes the environment. Then, the attenuation factor of the spin coherence (magnetization)  $\langle \sigma_x(t) \rangle = e^{-\mathcal{J}(x_B, t)}$  measured at time  $t$  is

$$\mathcal{J}(x_B, t) = \int_0^t dt' \int_0^{t'} dt'' g^2 \Phi(x_B, t'-t'') \Omega(t') \Omega^*(t''), \quad (\text{A7})$$



which can be cast in the spectral form

$$\mathcal{J}(x_B, t) = \int_{-\infty}^{\infty} d\omega F_t(\omega) G(x_B, \omega), \quad (\text{A8})$$

$$G(x_B, \omega) = \frac{1}{2\pi} \int_{-\infty}^{\infty} dt g^2 \Phi(x_B, t) e^{i\omega t}, \quad (\text{A9})$$

being the bath-coupling spectrum and

$$F_t(\omega) = \frac{1}{2\pi} \left| \int_0^t dt' \Omega(t') e^{i\omega t'} \right|^2 \quad (\text{A10})$$

is the filter function which depends on the dynamical control of the qubit probe.

We stress that  $\Omega(t)$  can have an *arbitrary* temporal shape, as opposed to the restrictions on its (*inherently pulsed*) shape in the dynamical decoupling method (Refs. [12,13,17,27] in the main text).

### Appendix B: Quantum Fisher information concerning a single parameter of the environment

The quantum Fisher information (QFI) concerning a single parameter  $x_B$  of the environment (bath) for the qubit state is [46, 47, 49]

$$\mathcal{F}_Q = \frac{1}{p_+} \left( \frac{\partial p_+}{\partial x_B} \right)^2 + \frac{1}{p_-} \left( \frac{\partial p_-}{\partial x_B} \right)^2 + 2 \frac{(p_+ - p_-)^2}{p_+ + p_-} \left( \left| \langle p_- | \frac{\partial |p_+\rangle}{\partial x_B} \right| + \left| \langle p_+ | \frac{\partial |p_-\rangle}{\partial x_B} \right| \right)^2, \quad (\text{B1})$$

where

$$p_{\pm}(x_B t) \equiv p(\pm |x_B, t) = \frac{1}{2} \left( 1 \pm e^{-\mathcal{J}(x_B, t)} \right), \quad (\text{B2})$$

$$|p_{\pm}\rangle = \frac{1}{\sqrt{2}} (e^{-i\omega_0 t} |\uparrow\rangle \pm |\downarrow\rangle)$$

are the eigenvalues and eigenvectors of the spin-probe density matrix [17, 74]. A measurement is said to be optimal when the QFI  $\mathcal{F}_Q$  coincides with its classical counterpart [46, 47, 49]. This is the case here under pure dephasing, when the last term in (B1) is null due to  $\frac{\partial |p_{\pm}\rangle}{\partial x_B} = 0$ . Then the optimal measurement is effected by projections onto the eigenstates  $|p_{\pm}\rangle$  of  $\sigma_x$  in the rotating frame

$$|p_{\pm}\rangle \langle p_{\pm}| = \frac{1}{2} e^{-i\frac{\omega_0}{2}\sigma_z} |\pm\rangle \langle \pm| e^{i\frac{\omega_0}{2}\sigma_z}, \quad (\text{B3})$$

$$|\pm\rangle = \frac{1}{\sqrt{2}} (|\uparrow\rangle \pm |\downarrow\rangle).$$

Correspondingly, Eq. (B1) becomes

$$\mathcal{F}_Q(x_B, t) = \frac{e^{-2\mathcal{J}(x_B, t)}}{1 - e^{-2\mathcal{J}(x_B, t)}} \left( \frac{\partial \mathcal{J}(x_B, t)}{\partial x_B} \right)^2, \quad (\text{B4})$$

if the initial probe-state is  $|+\rangle$ . An arbitrary initial state,  $(\cos(\theta)|\uparrow\rangle + i\sin(\theta)|\downarrow\rangle)$ ,  $0 < \theta < \frac{\pi}{2}$ , leads to  $\mathcal{F}_Q(x_B, t) \propto \sin^2(2\theta)$  [49]. Therefore, the optimal initial state leading to the maximal QFI is obtained for  $\theta = \frac{\pi}{4}$ ,  $|+\rangle = \frac{1}{\sqrt{2}} (|\uparrow\rangle + |\downarrow\rangle)$ , thus proving Eq. (6) in the main text.

### Appendix C: Derivation of the ultimate precision bound

A broad class of practically relevant environmental noise processes cause the attenuation factor to have a power-law functional dependence in  $x_B$  with exponent  $\alpha$ , where the derivative of  $\mathcal{J}(x_B, t)$  with respect to  $x_B$  satisfies

$$\left| \frac{\partial \mathcal{J}(x_B, t)}{\partial x_B} \right| \leq \frac{\alpha \mathcal{J}(x_B, t)}{x_B}. \quad (\text{C1})$$

The QFI then conforms to the inequality

$$\mathcal{F}_Q(x_B, t) \leq \frac{e^{-2\mathcal{J}(x_B, t)}}{1 - e^{-2\mathcal{J}(x_B, t)}} \frac{\alpha^2 \mathcal{J}(x_B, t)^2}{x_B^2}. \quad (\text{C2})$$

The equality is obtained when the attenuation factor is an homogeneous function of degree  $\alpha$ , i.e. strictly obeys a power law. The maximum of the QFI, regardless of the kind of control applied, is then obtained when  $\left| \frac{\partial \mathcal{J}(x_B, t)}{\partial x_B} \right| = \frac{\alpha \mathcal{J}(x_B, t)}{x_B}$  and  $\mathcal{J}(x_B, t) = \mathcal{J}_0 = 1 + \frac{1}{2}W(-2e^{-2}) \approx 0.8$ , where  $W(z)$  is the Lambert function which by definition satisfies  $z = W(z)e^{W(z)}$  for any complex number  $z$ . When the control is such that the equality in (C2) is satisfied, then the optimal total control-time at which the measurement should be done,  $t_{opt}$ , is such that  $\mathcal{J}(x_B, t_{opt}) = \mathcal{J}_0$ .

Under this condition, the resulting ultimate bound for the relative error in the estimation of  $x_B$ , which holds for arbitrary control on the probe, is

$$\varepsilon(x_B, t) \geq \frac{1}{x_B \sqrt{N_m \mathcal{F}_Q(x_B, t)}} \geq \frac{\sqrt{1 - e^{-2\mathcal{J}_0}}}{\alpha \sqrt{N_m} \mathcal{J}_0 e^{-\mathcal{J}_0}} = \frac{\varepsilon_0}{\alpha \sqrt{N_m}}, \quad (\text{C3})$$

with  $\varepsilon_0 = \sqrt{\frac{2}{-W(-2e^{-2})(1 + \frac{1}{2}W(-2e^{-2}))}} \approx 2.48$ .

#### 1. Precision bounds for the key parameters $g$ and $\tau_c$

##### (a) The probe-bath interaction strength $g$

The attenuation factor is an homogeneous function of degree  $\alpha = 2$  in the effective probe-bath interaction strength  $g$ , where  $G(\tau_c, \omega) = g^2 S(\omega)$  with  $S(\omega)$  the normalized spectral density of the environmental noise. Therefore, Eqs. (C1) and (C2) are satisfied and the minimal relative error in the estimation of  $g$  is obtained by measuring at the time  $t_{opt}$ , such that  $\mathcal{J}(g, t_{opt}) = \mathcal{J}_0$ , if  $S(\omega)$  is known.

(b) *The correlation time  $\tau_c$*

The derivative term in the QFI of Eq. (B4) depends on the derivative of the bath coupling-spectrum (spectral density) with respect to the correlation time  $\frac{\partial G}{\partial \tau_c}$ , through

$$\frac{\partial \mathcal{J}(\tau_c, t)}{\partial \tau_c} = \int_{-\infty}^{\infty} d\omega F_t(\omega) \frac{\partial G(\tau_c, \omega)}{\partial \tau_c}. \quad (\text{C4})$$

Spectral densities of the baths characterized by  $G_{\beta(s)}(\tau_c, \omega) = g^2 S(\omega)$  [defined in the main text, Eqs. (7-8)] satisfy  $\left| \frac{\partial S_{\beta(s)}}{\partial \tau_c} \right| \leq \frac{\alpha S_{\beta(s)}}{\tau_c}$ . Specifically,

$$\begin{aligned} \left| \frac{\partial G_{\beta}}{\partial \tau_c} \right| &= \left| \frac{\partial}{\partial \tau_c} \left( \frac{\mathcal{A}_{\beta} g^2 \tau_c}{1 + \omega^{\beta} \tau_c^{\beta}} \right) \right| \\ &= \left| \frac{\mathcal{A}_{\beta} g^2}{1 + \tau_c^{\beta} \omega^{\beta}} \left( 1 - \frac{\beta \tau_c^{\beta} \omega^{\beta}}{1 + \tau_c^{\beta} \omega^{\beta}} \right) \right| \\ &\leq \frac{\mathcal{A}_{\beta} g^2 (\beta - 1)}{(1 + \tau_c^{\beta} \omega^{\beta})} = \frac{(\beta - 1) G_{\beta}}{\tau_c} \end{aligned} \quad (\text{C5})$$

where the equality is attained when the spectral density function behaves as an homogeneous function of degree  $\alpha = \beta - 1$ ,  $G_{\beta} \propto \tau_c^{-(\beta-1)} \omega^{\beta}$ ; and

$$\frac{\partial G_s}{\partial \tau_c} = \frac{\partial}{\partial \tau_c} ((s+1) \tau_c^{s+1} \omega^s) = \frac{(s+1)}{\tau_c} G_s \quad (\text{C6})$$

since  $G_s$  is an homogeneous function of degree  $\alpha = s + 1$  upon neglecting the cutoff region.

Using Eqs. (C5-C6) to bound Eq. (C4), we find

$$\begin{aligned} \left| \frac{\partial \mathcal{J}(\tau_c, t)}{\partial \tau_c} \right| &= \int_{-\infty}^{\infty} d\omega F_t(\omega) \left| \frac{\partial G(\tau_c, \omega)}{\partial \tau_c} \right| \\ &\leq \frac{\alpha}{\tau_c} \int_{-\infty}^{\infty} d\omega F_t(\omega) G(\tau_c, \omega) \\ &= \frac{\alpha \mathcal{J}(\tau_c, t)}{\tau_c}. \end{aligned} \quad (\text{C7})$$

This leads to the tight bound for the Fisher information (C2) and therefore, for the minimal error in the estimation (C3) which holds for arbitrary control on the spin-probe. The ultimate bound in the precision (C3) is attained when the optimal total control-time at which the measurement should be done,  $t_{opt}$ , is such that  $\mathcal{J}(\tau_c, t_{opt}) = \mathcal{J}_0$ .

## Appendix D: Attainment of the ultimate bound

### 1. Attainment of the ultimate precision bound under optimal dynamical control in the estimation of key parameters:

(i) *Probe-bath interaction strength  $g$*

The attenuation factor is an homogeneous function of degree  $\alpha = 2$  in the probe-bath interaction strength  $g$ .

Therefore, Eqs. (C1) and (C2) are satisfied and the minimal relative error in the estimation of  $g$  is attained by measuring at a time  $t_{opt}$  such that  $\mathcal{J}(g, t_{opt}) = \mathcal{J}_0$  if  $S(\omega)$  is known.

If  $S(\omega)$  is not known, then some constraints apply for  $t_{opt}$ . Considering that the attenuation factor is given by (A8), then, if the filter function  $F_t(\omega)$  is much wider than  $G(g, \omega) = g^2 S(\omega)$ , it can be considered as a constant  $F_t$  in the integral (A8). The attenuation factor following the integration is then  $g^2 F_t$ , where we have used the normalization property of the spectral density  $S(\omega)$ . This limit holds when interval is shorter than the correlation time  $\tau_c$  of the environment, so that the qubit-probe evolves freely, yielding [15–17, 73, 74]

$$F_t^{free}(\omega) = \frac{t^2}{2} \text{sinc}^2(\omega t) \approx \frac{t^2}{2} \text{ if } t \ll \tau_c, \quad (\text{D1})$$

and

$$\mathcal{J}^{free}(g, t) \approx \frac{1}{2} g^2 t^2. \quad (\text{D2})$$

Then, the bound in the estimation error (C3) is achieved when

$$t_{opt}^{free} = \frac{\sqrt{2\mathcal{J}_0}}{g}, \text{ provided } t_{opt}^{free} = \sqrt{\frac{2\mathcal{J}_0}{g^2}} \ll \tau_c. \quad (\text{D3})$$

This condition can only be fulfilled for large enough  $\tau_c$ . To overcome this limitation, we may exploit dynamical control by means of frequent, stroboscopic quantum non-demolition (QND) measurements of the qubit-probe. If  $N$  QND *unread* measurements are performed during a total time  $t$ , the dynamics conforms to Zeno regime with an attenuation factor [15–17, 73, 74]

$$\mathcal{J}^{Zeno}(g, t) = \frac{g^2 t^2}{2N} \text{ if } \frac{t}{N} \ll \tau_c. \quad (\text{D4})$$

Then, the condition for attaining the bound in the estimation error (C3) is relaxed by  $1/\sqrt{N}$ , as

$$t_{opt}^{Zeno} = \frac{\sqrt{2N\mathcal{J}_0}}{g}, \text{ provided } \frac{t_{opt}^{Zeno}}{N} = \sqrt{\frac{2\mathcal{J}_0}{g^2 N}} \ll \tau_c. \quad (\text{D5})$$

The latter condition can be attained for

$$N \gg \frac{2\mathcal{J}_0}{g^2 \tau_c^2}. \quad (\text{D6})$$

In order to ensure that (A8) is satisfied, suffice it that the product  $g\tau_c$  be *roughly estimated*, by observing the change in the decay law from the anti-Zeno (AZE) or Fermi Golden Rule to the QZE regime as  $N$  increases [75].

(ii) *Correlation time  $\tau_c$*

Control of the spin-probe by  $N$ -pulse CPMG sequences or  $N$ -cycles of continuous-wave (CW) driving, leads to

a filter function  $F_t(\omega)$  that converges to a Fourier series described by a sum of delta functions (band narrow filters) centered at the harmonics of the inverse cycle time,  $k\omega_0 = \frac{\pi k N}{t}$   $k \in \mathbb{N}$ , provided the total control time exceeds the interval between the pulses  $t \gg \frac{t}{N}$ . Under these conditions, the attenuation factor (A8) becomes [23, 30]

$$\mathcal{J}(\tau_c, t) = g^2 \sum_{k=1}^{\infty} F_t(k\omega_0) G(\tau_c, k\omega_0). \quad (\text{D7})$$

In what follows we infer the conditions for attaining the bound from the attenuation factor for the bath spectra considered in the main text.

(1) For *generalized Ornstein-Uhlenbeck spectra*  $G_\beta$ , one condition to achieve the bound of Eq. (C3) is that the filter only overlap with the power-law tail spectra. This is ensured when the first harmonic of the filter is already in this spectral region, which amounts to  $\frac{t}{\pi N} \ll \tau_c$ . The attenuation factor (D7) then becomes

$$\mathcal{J}_\beta(\tau_c, t) = g^2 \sum_{k=1}^{\infty} F_t\left(\frac{\pi k N \tau_c}{t}\right) \frac{\mathcal{A}_\beta \tau_c}{\left(\frac{\pi k N \tau_c}{t}\right)^\beta} = \frac{c_\beta g^2 t^{\beta+1}}{N^\beta \tau_c^{\beta-1}}, \quad (\text{D8})$$

with  $\mathcal{A}_\beta = \frac{\beta}{2\pi} \sin(\frac{\pi}{\beta})$  and  $c_\beta = \frac{\beta}{2\pi^\beta} \sin(\frac{\pi}{\beta})$  for CW (only the first harmonic  $k = 1$  gives non-null terms) and  $c_\beta = \frac{\zeta(\beta+2)(4-2^{-\beta})\beta}{\pi^{2\beta}} \sin(\frac{\pi}{\beta})$  for CPMG (only odd  $k$  gives non-null terms) where  $\zeta$  is the zeta function defined for  $\text{Re}(z) > 1$  as  $\zeta(z) = \sum_{i=1}^{\infty} \frac{1}{i^z}$ . Both constants have similar values  $c_\beta^{CW} \approx c_\beta^{CPMG}$ .

Since  $\mathcal{J}_\beta$  satisfies the equality in Eq. (C2), the ultimate bound (C3) is achieved when  $\mathcal{J}_\beta(\tau_c, t_{opt}) = \mathcal{J}_0$ . This yields

$$t_\beta^{opt} = \tau_c^{\beta+1} \sqrt{\frac{N^\beta \mathcal{J}_0}{c_\beta g^2 \tau_c^2}}. \quad (\text{D9})$$

The resulting requirement on  $N$ , in order to keep the optimal narrowband approximation and overlap only with the power law tail

$$\frac{t^{opt}}{\pi N} \ll \tau_c, \quad \frac{t^{opt}}{\pi} \quad (\text{D10})$$

is then

$$N \gg \max \left\{ \frac{\mathcal{J}_0}{c_\beta g^2 \tau_c^2 \pi^{\beta+1}}, 1 \right\}. \quad (\text{D11})$$

If the control is constrained (say, by maximum total energy [26, 27, 76]), it may happen that the filter-function overlaps only with the Markovian region of the spectral density,  $G_\beta^M(\tau_c, \omega) \approx \mathcal{A}_\beta \tau_c$ , where it becomes a homogeneous function of order  $\alpha = 1$  on  $\tau_c$ . The attenuation factor is then independent of the dynamical control and is given by the Markovian limit

$$\mathcal{J}^M(\tau_c, t) = g^2 \tau_c t. \quad (\text{D12})$$

The ultimate bound (with  $\alpha = 1$ ) will then be achieved if the probe-state is measured at  $t_\beta^{M,opt} = \frac{\mathcal{J}_0}{g^2 \tau_c}$  independently of the control. This bound is always greater (worse) than the ultimate bound of Eq. (C3) for  $\beta > 2$ . For  $\beta = 2$ , where they are equal.

(2) For *generalized Ohmic spectra*  $G_s$ , the attenuation factor (D7) is

$$\begin{aligned} \mathcal{J}_s(\tau_c, t) &= g^2 \sum_{k=1}^{k_c} F_t\left(\frac{\pi k N \tau_c}{t}\right) (s+1) \tau_c^{(s+1)} \left(\frac{\pi k N \tau_c}{t}\right)^s \\ &= \frac{c_s g^2 \tau_c^{s+1} N^s}{t^{s-1}}, \end{aligned} \quad (\text{D13})$$

where  $c_s = \frac{\pi^{s+1}(s+1)}{2} \sum_{k=1}^{k_c} (2k-1)^{s-2}$  with  $k_c = \left\lceil \frac{t}{\pi N \tau_c} \right\rceil$  where the square brackets denote the integer part. Since the harmonics that contribute with non-null terms are those below the cutoff, then  $k_c$  is defined so as to satisfy  $\frac{\pi k_c N}{t} < \omega_c < \frac{\pi(k_c+1)N}{t}$  and therefore  $\frac{t}{\pi N \tau_c} + 1 < k_c < \frac{t}{\pi N \tau_c}$ .

The first requirement to achieve the bound (C3) is to avoid any overlap between the filter and the cutoff region, i.e.  $\frac{t}{\pi N k} \neq \tau_c$ , with  $k \in \mathbb{N}$ . This is most likely to be satisfied under the narrowband approximation that allows to design the filter to be null at cutoff.

The second requirement is that the filter should overlap with the power-law region. Therefore, one needs at least one harmonic below the cutoff that avoids the overlap with the cutoff, i.e.

$$\frac{t}{\pi N} > \tau_c. \quad (\text{D14})$$

Both conditions are ensured under CW control if  $\frac{t}{\pi N} > \tau_c$ , since the corresponding filter contains only one harmonic, leading to a simplified expression for the constant  $c_s = \frac{\pi^{s+1}(s+1)}{2}$ . Then,  $\mathcal{J}_s$  satisfies the equality in Eq. (C2) and the ultimate bound (C3) is achieved when  $\mathcal{J}_s(\tau_c, t_{opt}) = \mathcal{J}_0$ , yielding

$$t_s^{opt} = \tau_c^{s-1} \sqrt{\frac{c_s g^2 \tau_c^2 N^s}{\mathcal{J}_0}}. \quad (\text{D15})$$

To maintain this narrowband approximation, with one harmonic below the cutoff frequency, i.e.

$$\frac{t_s^{opt}}{\pi} \gg \frac{t_s^{opt}}{\pi N} > \tau_c, \quad (\text{D16})$$

the number of cycles  $N$  for super-Ohmic spectra ( $s > 1$ ) should satisfy

$$N_{superOhm} > \frac{\mathcal{J}_0 \pi^{s-1}}{c_s g^2 \tau_c^2} \text{ and } N_{superOhm} \gg 1 \quad (\text{D17})$$

and for sub-Ohmic spectra ( $0 < s < 1$ )

$$1 \ll N_{subOhm} < \frac{\mathcal{J}_0 \pi^{s-1}}{c_s g^2 \tau_c^2} \quad (\text{D18})$$

which is attainable when  $\sqrt{\frac{\mathcal{J}_0 \pi^{s-1}}{c_s}} \gg g\tau_c$ . For Ohmic spectra ( $s = 1$ )

$$1 \ll N_{Ohm} = \frac{\mathcal{J}_0}{c_s g^2 \tau_c^2} \quad (\text{D19})$$

implying that it must satisfy  $\sqrt{\frac{\mathcal{J}_0}{c_s}} \gg g\tau_c$ .

When the last conditions cannot be satisfied, less restrictive optimal solutions can be found by demanding the filter function to be null at the cutoff frequency  $\omega_c$ , and then finding the optimal control time.

(b) *The power law exponent*

To estimate the power law (PL) exponents  $s$  and  $\beta$  of spectral densities:  $G^{PL}(\omega) \propto \omega^s, \omega^{-\beta}$  or  $G(\omega) \propto \frac{1}{1+a\omega^a}$  with  $a = \text{const.}$ , we define the exponent  $x_B = \gamma$  that is common to both spectral densities:  $\gamma = 1 + \beta$  or  $\gamma = 1 - s$ , we note that the derivative of the attenuation factor with respect to the exponent satisfies (cf. Eqs. (1), (4) in the main text)

$$\begin{aligned} \left| \frac{\partial \mathcal{J}(x_B = \gamma, t)}{\partial \gamma} \right| &= \left| \int_{-\infty}^{\infty} d\omega F_t(\omega) \frac{\partial G(\gamma, \omega)}{\partial \gamma} \right| \quad (\text{D20}) \\ &\leq \left| \int_{-\infty}^{\infty} d\omega F_t(\omega) \frac{\partial G^{PL}(\gamma, \omega)}{\partial \gamma} \right| \\ &= \left| \frac{\partial \mathcal{J}^{PL}(\gamma, t)}{\partial \gamma} \right|. \end{aligned}$$

This expression tightly bound the QFI (B4). To attain the ultimate bound for the relative error of the estimation by the maximized QFI, one needs to apply a control that only probes the power-law regime of the spectral density. The attenuation factor under such control can be expressed as  $\mathcal{J}(\gamma, t) = \mathcal{J}^{PL}(\gamma, t) = \left(\frac{t}{T_2}\right)^\gamma$ , where the dephasing time  $T_2$  depends on the applied control. Then,

$$\left| \frac{\partial \mathcal{J}(\gamma, t)}{\partial \gamma} \right| = \frac{\mathcal{J}(\gamma, t)}{\gamma} |\ln(\mathcal{J}(\gamma, t))| \quad (\text{D21})$$

and the ultimate precision bound in the estimation is then given by Eq. (13) of the main text. The bound is achieved when the qubit-probe is measured at  $t_{opt} = T_2 \sqrt[3]{\mathcal{J}_1}$  with  $\mathcal{J}_1 = e^{-2.246} \approx 0.106$  when the dynamical control can ensure this regime. For example, under CW or CPMG control for estimating the power law of an Ornstein-Uhlenbeck process, the time interval between the number of pulses should be smaller than the correlation time,  $\frac{t_{opt}}{N} \ll \tau_c$ , so that  $N \gg \frac{T_2 \sqrt[3]{\mathcal{J}_1}}{\tau_c}$ .

(c) *Unattainability of the ultimate bound under free evolution (free-induction decay - FID)*

We here discuss the unattainability of the ultimate precision bound when the spin-probe evolves freely, for the

estimation of:

(i) *probe-bath interaction strength  $g$*  (the conditions to attain the relevant bound are discussed in the main text starting with Eqs. (D1) and ending in Eqs. (D3)), and

(ii) *the correlation time  $\tau_c$* , for which, as observed in Fig. 2 of the main text, the estimation precision becomes worse as  $g\tau_c$  grows. For the generalized Ornstein-Uhlenbeck spectra  $G_\beta$ , as discussed in the main text, the free-evolution filter  $F_t^{free}(\omega)$ , Eq. (D1), overlaps with the  $\omega \approx 0$  region and consequently the equality in Eq. (C5) cannot be fulfilled. For the generalized Ohmic spectra  $G_s$ , when  $t \ll \tau_c$ , one can approximate Eq. (A8) by its zero-order term, considering that  $F_t^{free}(\omega)$  is independent of  $\omega$ , since  $G(\tau_c, \omega)$  is much narrower than  $F_t^{free}(\omega)$ .

The attenuation factor in this regime becomes independent of  $\tau_c$ , as in Eq. (D2),  $\mathcal{J}_\beta^{free}(\tau_c, t) = \mathcal{J}_s^{free}(\tau_c, t) \approx \frac{1}{2} g^2 t^2$ . In this regime there is no information concerning the correlation time  $\tau_c$ . If  $\frac{1}{2} g^2 \tau_c^2 \gg \mathcal{J}_0$ , then it will not be possible to achieve the bound under free evolution. The attenuation factor will depend on  $\tau_c$  only when  $t \gtrsim \tau_c$ , and therefore  $\frac{1}{2} g^2 t^2 \gtrsim \frac{1}{2} g^2 \tau_c^2 \gg \mathcal{J}_0$ , implying that the ultimate bound on Eq. (C3) cannot be achieved.

The limitation of the estimation of  $\tau_c$  for the spectra  $G_s$  using freely evolving spin-probes is that the only control parameter is the time  $t$  that may not simultaneously avoid the overlap of the filter function with  $\omega_c$  and render the attenuation factor equal to  $\mathcal{J}_0$ , *i.e.* usually  $t_{opt} \neq 4\pi n \tau_c$ ,  $n \in \mathbb{N}$ . Hence, the ultimate bound is generally not achieved under free evolution.

(d) *Pulse-error effects*

In the preceding analysis, we have considered ideal, *i.e.* perfect and stroboscopic, pulses. If non-ideal pulse-effects are important, one needs a model for their effect on the dephasing. Typically the pulses are applied with the same phase, as in CPMG, where flip-angle errors are compensated and the pure dephasing assumption is still suitable [30, 77]. In this case, if finite-width pulse effects are significant, they can be considered by modifying the effective filter functions [78]. Therefore, within this model for the error effects, our ultimate bound is valid and achievable in the presence of such pulse-error effects. If pulse imperfections generate an effective Hamiltonian that deviates from a pure dephasing [77, 79], then a different approach to calculate the ultimate bound must be pursued. However, for parameter estimation, control pulses with good fidelity are essential. Alternatively, one may have to resort to more elaborate controls, nicknamed by us “selective dynamical recoupling” (SDR), which we have shown to allow *selective* probing of the targeted noise source by factoring out uncontrollable noise sources, such as an intrinsic  $T_2$  decoherence due to a white-noise (Markovian) process or due to pulse imperfections [10, 11].

### Appendix E: Information gain for the real-time adaptive estimation protocol

The best *total control and measurement time*  $t'$  to be chosen for the next iteration of the real-time estimation protocol are determined by the averaged information gain from the currently available probability distribution of  $x_B$ ,  $p(x_B|d, t)$ , assuming that *experimental outcome*  $d$  was obtained in the iteration measured at  $t$  [56].

The expected probability to obtain the outcome  $d'$  by measuring the controlled spin-probe at time  $t'$  from the current probability distribution of  $x_B$  is

$$p(d'|t', d, t) = \int p(d'|x_B, t)p(x_B|d, t)d\tau_c. \quad (\text{E1})$$

The total information gain of a measurement at time  $t'$  is given by

$$U(t') = \sum_{d'} p(d'|t', d, t)U(d', t'), \quad (\text{E2})$$

where  $U(d', t')$  is the information gain if the measurement at  $t'$  gives the result  $d'$ .

The information gain of an outcome, according to information theory, is measured by the entropy

$$U(d', t') = \int p(x_B|d', t', d, t)\log(p(x_B|d', t', d, t))dx_B. \quad (\text{E3})$$

Then, the best time for the next control/measurement  $t_m$  is defined by the value that maximizes the expected information

$$U(t_m) = \max_{t'} \left\{ \sum_{d'} p(d'|t', d, t) \int p(x_B|d', t', d, t)\log(p(x_B|d', t', d, t)) dx_B \right\} \quad (\text{E4})$$

$$(\text{E5})$$

### Acknowledgments

We thank L. Frydman and N. Shemesh for fruitful discussions. G.A.A. acknowledges the support of the European Commission under the Marie Curie Intra-European Fellowship for Career Development grant no. PIEF-GA-2012-328605. G.K. acknowledges the ISF support under the Bikura (Prime) grant.

- 
- [1] J. M. Taylor, P. Cappellaro, L. Childress, L. Jiang, D. Budker, P. R. Hemmer, A. Yacoby, R. Walsworth, and M. D. Lukin, *Nat. Phys.* **4**, 810 (2008).
- [2] G. Balasubramanian, I. Y. Chan, R. Kolesov, M. Al-Hmoud, J. Tisler, C. Shin, C. Kim, A. Wojcik, P. R. Hemmer, A. Krueger, T. Hanke, A. Leitenstorfer, R. Bratschitsch, F. Jelezko, and J. Wrachtrup, *Nature* **455**, 648 (2008).
- [3] G. Kucsko, P. C. Maurer, N. Y. Yao, M. Kubo, H. J. Noh, P. K. Lo, H. Park, and M. D. Lukin, *Nature* **500**, 54 (2013).
- [4] P. Neumann, I. Jakobi, F. Dolde, C. Burk, R. Reuter, G. Waldherr, J. Honert, T. Wolf, A. Brunner, J. H. Shim, D. Suter, H. Sumiya, J. Isoya, and J. Wrachtrup, *Nano Lett.* **13**, 2738 (2013).
- [5] D. M. Toyli, C. F. d. I. Casas, D. J. Christle, V. V. Dobrovitski, and D. D. Awschalom, *Proc. Natl. Acad. Sci. U. S. A.* **110**, 8417 (2013).
- [6] S. Steinert, F. Ziem, L. T. Hall, A. Zappe, M. Schweikert, N. Götz, A. Aird, G. Balasubramanian, L. Hollenberg, and J. Wrachtrup, *Nat. Commun.* **4**, 1607 (2013).
- [7] M. S. Grinolds, M. Warner, K. D. Greve, Y. Dovzhenko, L. Thiel, R. L. Walsworth, S. Hong, P. Maletinsky, and A. Yacoby, *Nat. Nanotechnol.* **9**, 279 (2014).
- [8] A. Sushkov, I. Lovchinsky, N. Chisholm, R. Walsworth, H. Park, and M. Lukin, *Phys. Rev. Lett.* **113**, 197601 (2014).
- [9] A. Mittermaier and L. Kay, *Science* **312**, 224 (2006).
- [10] P. E. S. Smith, G. Bensky, G. A. Álvarez, G. Kurizki, and L. Frydman, *Proc. Natl. Acad. Sci. U. S. A.* **109**, 5958 (2012).
- [11] G. A. Álvarez, N. Shemesh, and L. Frydman, *Phys. Rev. Lett.* **111**, 080404 (2013).
- [12] W. Zurek, *Rev. Mod. Phys.* **75**, 715 (2003).
- [13] L. Viola, E. Knill, and S. Lloyd, *Phys. Rev. Lett.* **82**, 2417 (1999).
- [14] L. Viola, S. Lloyd, and E. Knill, *Phys. Rev. Lett.* **83**, 4888 (1999).
- [15] A. G. Kofman and G. Kurizki, *Phys. Rev. Lett.* **87**, 270405 (2001).
- [16] A. G. Kofman and G. Kurizki, *Phys. Rev. Lett.* **93**, 130406 (2004).
- [17] G. Gordon, N. Erez, and G. Kurizki, *J. Phys. B: At. Mol. Opt. Phys.* **40**, S75 (2007).
- [18] K. Khodjasteh and D. Lidar, *Phys. Rev. Lett.* **95**, 180501 (2005).
- [19] A. M. Souza, G. A. Álvarez, and D. Suter, *Phil. Trans. R. Soc. A* **370**, 4748 (2012).
- [20] C. A. Meriles, L. Jiang, G. Goldstein, J. S. Hodges, J. Maze, M. D. Lukin, and P. Cappellaro, *J. Chem. Phys.* **133**, 124105 (2010).
- [21] I. Almog, Y. Sagi, G. Gordon, G. Bensky, G. Kurizki, and N. Davidson, *J. Phys. B: At., Mol. Opt. Phys.* **44**, 154006 (2011).

- [22] J. Bylander, S. Gustavsson, F. Yan, F. Yoshihara, K. Harrabi, G. Fitch, D. G. Cory, Y. Nakamura, J. Tsai, and W. D. Oliver, *Nat. Phys.* **7**, 565 (2011).
- [23] G. A. Álvarez and D. Suter, *Phys. Rev. Lett.* **107**, 230501 (2011).
- [24] C. O. Bretschneider, G. A. Álvarez, G. Kurizki, and L. Frydman, *Phys. Rev. Lett.* **108**, 140403 (2012).
- [25] L. Cywinski, *Phys. Rev. A* **90**, 042307 (2014).
- [26] J. Clausen, G. Bensky, and G. Kurizki, *Phys. Rev. Lett.* **104**, 040401 (2010).
- [27] G. Gordon, G. Kurizki, and D. A. Lidar, *Phys. Rev. Lett.* **101**, 010403 (2008).
- [28] H. Uys, M. J. Biercuk, and J. J. Bollinger, *Phys. Rev. Lett.* **103**, 040501 (2009).
- [29] K. Khodjasteh, D. A. Lidar, and L. Viola, *Phys. Rev. Lett.* **104**, 090501 (2010).
- [30] A. Ajoy, G. A. Álvarez, and D. Suter, *Phys. Rev. A* **83**, 032303 (2011).
- [31] D. Hayes, K. Khodjasteh, L. Viola, and M. J. Biercuk, *Phys. Rev. A* **84**, 062323 (2011).
- [32] V. Mukherjee, A. Carlini, A. Mari, T. Caneva, S. Montangero, T. Calarco, R. Fazio, and V. Giovannetti, *Phys. Rev. A* **88**, 062326 (2013).
- [33] K. Khodjasteh, J. Sastrawan, D. Hayes, T. J. Green, M. J. Biercuk, and L. Viola, *Nat. Commun.* **4** (2013), 10.1038/ncomms3045.
- [34] G. Gordon and G. Kurizki, *New J. Phys.* **10**, 045005 (2008).
- [35] K. Khodjasteh and L. Viola, *Phys. Rev. Lett.* **102**, 080501 (2009).
- [36] G. A. Paz-Silva, A. T. Rezakhani, J. M. Dominy, and D. A. Lidar, *Phys. Rev. Lett.* **108**, 080501 (2012).
- [37] C. Kabytayev, T. J. Green, K. Khodjasteh, M. J. Biercuk, L. Viola, and K. R. Brown, *Phys. Rev. A* **90**, 012316 (2014).
- [38] G. A. Álvarez, M. Mishkovsky, E. P. Danieli, P. R. Levstein, H. M. Pastawski, and L. Frydman, *Phys. Rev. A* **81**, 060302 (R) (2010).
- [39] A. Zwick, G. A. Álvarez, G. Bensky, and G. Kurizki, *New J. Phys.* **16**, 065021 (2014).
- [40] A. Ajoy and P. Cappellaro, *Phys. Rev. Lett.* **110**, 220503 (2013).
- [41] D. Petrosyan, G. Bensky, G. Kurizki, I. Mazets, J. Majer, and J. Schmiedmayer, *Phys. Rev. A* **79**, 040304 (2009).
- [42] G. Bensky, D. Petrosyan, J. Majer, J. Schmiedmayer, and G. Kurizki, *Phys. Rev. A* **86**, 012310 (2012).
- [43] N. Shemesh, G. A. Álvarez, and L. Frydman, *J. Magn. Reson.* **237**, 49 (2013).
- [44] H. J. Mamin, M. Kim, M. H. Sherwood, C. T. Retner, K. Ohno, D. D. Awschalom, and D. Rugar, *Science* **339**, 557 (2013).
- [45] T. Staudacher, F. Shi, S. Pezzagna, J. Meijer, J. Du, C. A. Meriles, F. Reinhard, and J. Wrachtrup, *Science* **339**, 561 (2013).
- [46] S. Braunstein and C. Caves, *Phys. Rev. Lett.* **72**, 3439 (1994).
- [47] M. G. A. Paris, *International Journal of Quantum Information* **07**, 125 (2009).
- [48] B. M. Escher, R. L. de Matos Filho, and L. Davidovich, *Nat. Phys.* **7**, 406 (2011).
- [49] C. Benedetti and M. G. A. Paris, arXiv:1406.7610v1 [quant-ph] (2014).
- [50] A. G. Kofman and G. Kurizki, *Nature* **405**, 546 (2000).
- [51] N. Bar-Gill, L. M. Pham, C. Belthangady, D. L. Sage, P. Cappellaro, J. R. Maze, M. D. Lukin, A. Yacoby, and R. Walsworth, *Nat. Commun.* **3**, 858 (2012).
- [52] J. Medford, L. Cywiński, C. Barthel, C. M. Marcus, M. P. Hanson, and A. C. Gossard, *Phys. Rev. Lett.* **108**, 086802 (2012).
- [53] Y. Romach, C. Müller, T. Unden, L. J. Rogers, T. Isoda, K. M. Itoh, M. Markham, A. Stacey, J. Meijer, S. Pezzagna, B. Naydenov, L. P. McGuinness, N. Bar-Gill, and F. Jelezko, *Phys. Rev. Lett.* **114**, 017601 (2015).
- [54] D. Suter and R. R. Ernst, *Phys. Rev. B* **32**, 5608 (1985).
- [55] A. Feintuch, A. Grayevsky, N. Kaplan, and E. Dormann, *Phys. Rev. Lett.* **92**, 156803 (2004).
- [56] C. E. Granade, C. Ferrie, N. Wiebe, and D. G. Cory, *New J. Phys.* **14**, 103013 (2012).
- [57] A. Sergeevich, A. Chandran, J. Combes, S. Bartlett, and H. Wiseman, *Phys. Rev. A* **84**, 052315 (2011).
- [58] M. D. Shulman, S. P. Harvey, J. M. Nichol, S. D. Bartlett, A. C. Doherty, V. Umansky, and A. Yacoby, *Nat. Commun.* **5** (2014).
- [59] P. Cappellaro, *Phys. Rev. A* **85**, 030301 (2012).
- [60] H.-P. Breuer and F. Petruccione, *The Theory of Open Quantum Systems* (Oxford University Press, 2007).
- [61] G. A. Álvarez, D. D. B. Rao, L. Frydman, and G. Kurizki, *Phys. Rev. Lett.* **105**, 160401 (2010).
- [62] C. P. Slichter, *Principles of Magnetic Resonance* (Springer Berlin Heidelberg, Berlin, Heidelberg, 1990).
- [63] G. A. Álvarez, R. Kaiser, and D. Suter, *Ann. Phys. (Berlin)* **525**, 833 (2013).
- [64] C. Joachim, J. K. Gimzewski, and A. Aviram, *Nature* **408**, 541 (2000).
- [65] G. Ithier, E. Collin, P. Joyez, P. Meeson, D. Vion, D. Esteve, F. Chiarello, A. Shnirman, Y. Makhlin, J. Schrieffer, and G. Schön, *Phys. Rev. B* **72**, 134519 (2005).
- [66] G. A. Álvarez, N. Shemesh, and L. Frydman, *J. Chem. Phys.* **140**, 084205 (2014).
- [67] V. Giovannetti, S. Lloyd, and L. Maccone, *Phys. Rev. Lett.* **96**, 010401 (2006).
- [68] R. Demkowicz-Dobrzański and L. Maccone, *Phys. Rev. Lett.* **113**, 250801 (2014).
- [69] S. F. Huelga, C. Macchiavello, T. Pellizzari, A. K. Ekert, M. B. Plenio, and J. I. Cirac, *Phys. Rev. Lett.* **79**, 3865 (1997).
- [70] G. Gordon and G. Kurizki, *Phys. Rev. Lett.* **97**, 110503 (2006).
- [71] G. Gordon and G. Kurizki, *Phys. Rev. A* **83**, 032321 (2011).
- [72] M. Tsang, H. M. Wiseman, and C. M. Caves, *Phys. Rev. Lett.* **106**, 090401 (2011).
- [73] A. G. Kofman and G. Kurizki, *IEEE Trans. Nanotechnology* **4**, 116 (2005).
- [74] G. Gordon, *J. Phys. B: At. Mol. Opt. Phys.* **42**, 223001 (2009).
- [75] D. D. Bhaktavatsala Rao and G. Kurizki, *Phys. Rev. A* **83**, 032105 (2011).
- [76] J. Clausen, G. Bensky, and G. Kurizki, *Phys. Rev. A* **85**, 052105 (2012).
- [77] G. A. Álvarez, A. Ajoy, X. Peng, and D. Suter, *Phys. Rev. A* **82**, 042306 (2010).
- [78] M. J. Biercuk, H. Uys, A. P. VanDevender, N. Shiga, W. M. Itano, and J. J. Bollinger, *Phys. Rev. A* **79**, 062324 (2009).
- [79] K. Khodjasteh and D. A. Lidar, *Phys. Rev. A* **75**, 062310 (2007).